Chemical Mimicry: Hierarchical 1D TiO 2 @ZrO 2 Core–Shell Structures Reminiscent of Sponge Spicules by the Synergistic Effect of Silicatein-α and Silintaphin-1

ARTICLE *in* LANGMUIR · APRIL 2011

Impact Factor: 4.46 · DOI: 10.1021/la200066q · Source: PubMed

Langmuir

ARTICLE

pubs.acs.org/Langmuir

Chemical Mimicry: Hierarchical 1D TiO_2@ZrO_2 Core−Shell Structures Reminiscent of Sponge Spicules by the Synergistic Effect of Silicatein-α and Silintaphin-1

Rute André,[†] Muhammad Nawaz Tahir,[†] Thorben Link,[§] Florian D. Jochum,[‡] Ute Kolb,[∥] Patrick Theato,[‡] Rüdiger Berger,[⊥] Matthias Wiens,[§] Heinz-Christoph Schröder,[§] Werner E. G. Müller,[§] and Wolfgang Tremel*[,†]

[†]Institut für Anorganische Chemie und Analytische Chemie, [‡]Institut für Organische Chemie, and [§]Institut für Physiologische Chemie, Johannes Gutenberg-Universität, Duesbergweg 10-14, D-55099 Mainz, Germany

[∥]Institut für Physikalische Chemie, Johannes Gutenberg-Universität, Welderweg 15, D-55099 Mainz, Germany

[⊥]Max Planck-Institut für Polymerforschung, Ackermannweg 10, D-55128 Mainz, Germany

Supporting Information

ABSTRACT: In nature, mineralization of hard tissues occurs due to the synergistic effect of components present in the organic matrix of these tissues, with templating and catalytic effects. In *Suberites domuncula*, a well-studied example of the class of demosponges, silica formation is mediated and templated by an axial proteinaceous filament with silicatein-α, one of the main components. But so far, the effect of other organic constituents from the proteinaceous filament on the catalytic effect of silicatein-α has not been studied in detail. Here we describe the synthesis of core−shell TiO_2@SiO_2 and TiO_2@ZrO_2 nanofibers via grafting of silicatein-α onto a TiO_2 nanowire backbone followed by a coassembly of silintaphin-1 through its specifically interacting domains. We show for the first time a linker-free, one-step funtionalization of metal oxides with silicatein-α using glutamate tag. In the presence of silintaphin-1 silicatein-α facilitates the formation of a dense layer of SiO_2 or ZrO_2 on the TiO_2@protein backbone template. The immobilization of silicatein-α onto TiO_2 probes was characterized by atomic force microscopy (AFM), optical light microscopy, and high-resolution transmission electron microscopy (HRTEM). The coassembly of silicatein-α and silintaphin-1 may contribute to biomimetic approaches that pursue a controlled formation of patterned biosilica-based biomaterials.

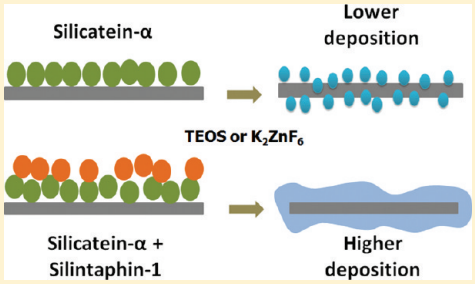

INTRODUCTION

Controlling the surface binding, distribution, and targeting of nanoparticles is a key requirement for the technology to use them in applications.[1,2] Utilizing the special properties of nanoparticles, such as mechanical, optical, or magnetic ones, depends on our means of positioning and organizing them in a functional context. For this, self-assembly is a very attractive strategy. Ideally, the components contain in their structures the information needed for finding their correct place and position to build functional assemblies.[3−6] Self-assembly is ubiquitous in biology, where numerous examples have been studied in much detail, and it is a challenge for current technology to make use of self-assembly in manufacturing materials, electronics, devices, etc.[7,8]

As self-assembly is essential to biology at the molecular scale, it is interesting to turn to biology for understanding and inspiration.[9] In nature, hard tissues are formed typically by composite materials that exhibit multiple levels of hierarchical organization and complex architectures.[10,11] This structural hierarchy can play a major role in determining the bulk material properties.[12] Understanding the growth of these hierarchical structures in vivo can guide the synthesis of new materials in vitro with improved physical properties and tailored for specific applications.[12−14] One example is the hierarchically ordered mineral skeleton of some marine sponges, like *Euplectella* sp.[15] In some siliceous sponges (demosponges and hexactinellids), silica is deposited around an organic, axial filament formed by several different proteins, like galactins, lectins, collagen, different isoforms of silicatein (α, β, and γ), silintaphin, among other components still under study. All these components have different functions, from the catalytic formation of silica (like silicatein) to templating (collagen) and structure guiding (silintaphin) of the final spicule structure.[16−18] The needlelike spicules formed in this way have a lamellar structure resulting in an organic−inorganic composite.[19] Spicule formation in some of the demosponges starts within the cell and then proceeds outside the cell.[20,21] The spicule growth proceeds in a radial fashion.

Received: January 6, 2011
Revised: February 23, 2011
Published: April 01, 2011

We could demonstrate that the appositional formation of silica lamellae around the spicules is preceded by the formation of hollow cylinders, formed by matrix-guided silicatein, which mediates biocatalytic synthesis and deposition of nanostructured silica.[16] It has been demonstrated that silicatein-α mediates not only the synthesis of biosilica but also the formation of other metal oxides such as titania (TiO_2),[22−24] zirconia (ZrO_2),[24] and GaOOH/spinel gallium oxide,[25] among others, from water stable precursors at room temperature and neutral pH, whereas the chemical synthesis of these materials requires acidic pH and elevated temperatures. Such flexibility in uptaking different substrates makes silicatein a very atractive tool for new material synthesis in mild conditions and as an inspirational tool for development of other biomimetic small molecules.[26]

The organic−inorganic assembly in biocomposite materials provides them with unique property combinations. Sponge spicules combine mechanical strength with excellent optical properties. Sponge spicules exhibit advantageous properties compared to materials offered by engineering, such as technical optical fibers,[27,28] based on their composite structure and their lamellar architecture, resulting in enhanced fracture toughness, as well as their low-temperature synthesis and the presence dopants (sodium), raising the refractive index of the fibers. The process of silica deposition in the some siliceous sponges is enzymatically mediated and matrix-guided.[20,29,30] As mentioned above, not only the enzyme silicatein, in its different isoforms, is present in the axial filament of these sponges but also many other proteins. Very often proteins must bind to other specific proteins in vivo in order to function. The proteins are required to bind to only one or a few other proteins of the few thousand proteins typically present in vivo.[31−33] In the exemplified sponge spicules, this case is not an exception, as recently a new protein was isolated from the spicule axial filament, silintaphin-1, which is believed to act through its sticky domains as a scaffold/backbone for silicatein binding and assembly.[18]

One intriguing question is whether the hierarchical mineral skeleton that is encountered in sponge spicules can be modeled synthetically through a layer-by-layer deposition of inorganic nanoparticles on a soft polymer or rigid inorganic backbone template. In this contribution, we address the question whether a concentric layer of silica nanoparticles can be deposited in a biomimetic manner using surface-immobilized silicatein as a hydrolytic catalyst. We have demonstrated previously that recombinant silicatein[34] retains its biocatalytic activity after immobilization onto metal oxide surfaces.[35,36] His-tagged silicatein was immobilized in self-assembled monolayeres (SAMs) on Au(111) with nitrilotriacetic acid (NTA) terminated thiols, which bind to the His-tag chelating anchor through Ni^{2+} complexation.[35] The recombinant protein, bound through a His-tag affinity sequence to the chelator NTA, was able to catalyze the formation of silica nanospheres with diameters of 70−300 nm. The principle of binding silicatein molecules to a self-assembled polymer layer was applied for the preparation of functional spicule-like core−shell materials with (alternating) metal oxide layers. Using this approach we could immobilize silicatein not only onto the surface of isolated spicules to synthesize new silica lamellae[37] but also on the surface of magnetic oxide nanoparticles to generate silica coatings by the immobilized enzyme.[38] Such particles are of extreme interest for targeting cell surface receptors and for protein separation.[39,40]

In order to reduce the number of nonbiocompatible reaction steps, silicatein was immobilized, in this work, onto titania nanowires with a glutamate-tag in the c-terminus of silicatein-α. The glutamate tag in silicatein-α was shown before to allow a specific binding of silicatein to hydroxyapatite.[41] An improvement of the morphological control over the polymerized silica layer could be achieved with the aid of silintaphin-1, which binds specifically and strongly to the immobilized silicatein-α in vitro.[18] This conjugated matrix still allows silicatein to be active toward the formation of silica and other metal oxides (e.g., zirconia). The difference in the oxide coatings with only silicatein and with silicatein/silintaphin-1 was also tested, showing that a denser organic matrix allows for an increased deposition of oxides, even though silintaphin-1 itself is not catalytically active. We anticipate that the model method described here can be generalized using other metal oxide nanostructures, allowing the synthesis of a wide range of nanocomposite materials under physiological conditions.

EXPERIMENTAL SECTION

Methods and Materials. Titanium isopropoxide (ACROS, 99%), tetraethyl orthosilicate (TEOS, Sigma-Aldrich, 99.9%), potassium hexafluorozirconate (K_2ZrF_6, Sigma-aldrich, 99%), Tris-buffered saline (TBS, Sigma-aldrich), milk powder (Carl Roth), Cy3-conjugated goat antirabbit antibody (Dianova), and AlexaFluor488 conjugated antimouse antibody (Invitrogen) were purchased and used as received without further purification. Solvents, acids, and bases, such as ethanol, dichloromethane, HCl, HNO_3, and NaOH, were purchased technical grade and used as received.

Synthesis of the TiO_2 Nanowires. The TiO_2 nanowires were synthesized following a modified procedure given by Bruce and co-workers.[42] In brief, 1 g of titanium isopropoxide was taken in a Teflon vessel and 6 mL of analytical grade ethanol (99.8%) was added into it. The Teflon vessel was kept in a desiccator. The precipitation of TiO_2 was initiated under a moist atmosphere induced by placing a Petri dish filled with water at the bottom of the desiccator. The diffusion experiment was stopped after 12 h, followed by the addition of 25 mL of 10 M NaOH aqueous solution. Then the reaction vessel was sealed into a stainless steel hydrothermal bomb, which was placed in an oven maintained at 180 °C for 20 h. The obtained sample was filtered and repeatedly washed with 0.1 M HNO_3, 1 N HCl, and deionized water. The product was dried under vacuum for 3 h. Further details concerning the characterization of the nanowires are given in the Supporting Information.

Glu-Tagged Silicatein-α and Silintaphin-1 Immobilization. Recombinant glutamate-tagged silicatein-α and silintaphin-1 were prepared as described before.[18,41] For the functionalization of silicatein, 1 mg of TiO_2 nanowires was dispersed and sonicated in 5 mL of TBS buffer (pH 7.4) until they were totally dispersed. Subsequently, silicatein-α was added in order to obtain a final concentration of 30 nmol. Different incubation times between 1 and 5 h were tested for the enzymes. As agglomerates were formed after 2 h, most reactions were carried out for 1 h or 2 h. The sample was incubated at room temperature for 2 h with agitation. The Glu-tagged silicatein-α immobilized TiO_2 nanowires were washed with TBS buffer (pH 7.4) to remove unbound protein. To further immobilize silintaphin-1, a solution of 30 nmol of protein in TBS buffer (pH 7.4) was added to the silicatein-functionalized TiO_2 nanowires, incubating for 1 h with agitation.[18] Then the sample was washed with buffer to remove unbound protein. Prior to use all samples were resuspended in TBS buffer (pH 7.4).

Immunostaining and Confocal Imaging. Specific antisilicatein and antisilintaphin antibodies were prepared as described before.[34,18] The immobilization of silicatein and silintaphin was monitored by incubating primary antisilicatein (produced in rabbit) or antisilintaphin (produced in mouse) polyclonal antibody (1:2000 dilution), in a 5% blocking solution (milk powder) for 2 h at room temperature. The sample was washed several times using TBS (Tris-buffered saline, pH 7.4) for 5 min followed by the secondary antibody, antirabbit Cy3 labeled or antimouse AlexaFluor

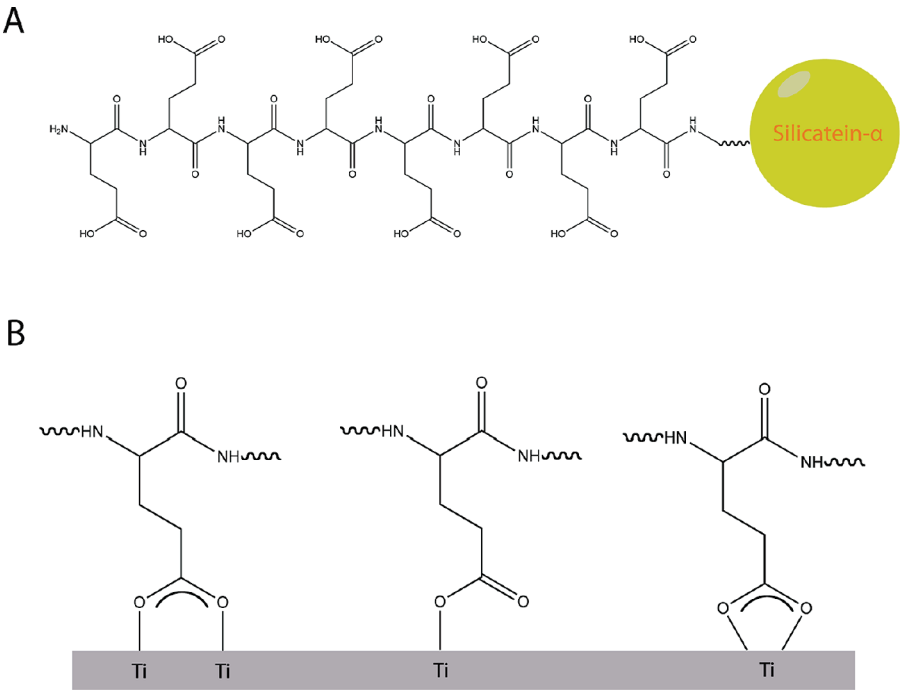

Figure 1. Modified silicatein-α with an eight glutamate tags (A) and different possible binding modes of glutamate to a titania surface (B). Schemes are not to scale.

488 labeled (1:2000 dilution), for silicatein-α and silintaphin-1, respectively, incubated in 5% blocking solution for 3 h at room temperature, and then washed with TBS. As a control, TiO_2 nanowires without immobilized protein were used. The fluorescence analysis was performed with an Olympus AHBT3 light microscope, together with an AH3-RFC-reflected light fluorescence attachment at the emission wavelength of 580 and 499 nm.

Protein-Assisted Synthesis of Silica and Zirconia. For the deposition of silica or zirconia, TiO_2 nanowires functionalized with just Glu-tagged silicatein-α or with both silicatein and silintaphin were used. In all experiments, for the silica synthesis, the TiO_2 nanowires were incubated with a 5 mM solution of TEOS in TBS buffer (pH 7.4) for 5 h at room temperature with agitation. For the zirconia synthesis, the TiO_2 nanowires were incubated with a 5 mM solution of K_2ZnF_6 in TBS buffer (pH 7.4) for 5 h at room temperature with agitation. After incubation, the nanowires were washed with Milli-Q water and ethanol several times and dried under a stream of N_2.

As a control, nanowires with silintaphin-1 directly immobilized were used. Further details regarding the functionalization can be found in the Supporting Information. The silintaphin-1-functionalized nanowires were incubated under the same conditions as above with TEOS or K_2ZrF_6, where no catalytic effect was observed.

Transmission Electron Microscopy. Characterization and morphology analysis of the samples were carried out using transmission electron microscopy (TEM) using a Philips 420 instrument with an acceleration voltage of 120 kV or, for high-resolution TEM, a Philips TECNAI F30 electron microscope (field-emission gun, 300 kV extraction voltage). The samples for TEM analysis were first washed with Milli-Q water and ethanol to remove the possible buffer salts. Afterward, 5 μL of the products resuspended in ethanol were drop-cast in TEM grids covered with carbon and allowed to dry overnight at room temperature, before analysis.

Thickness and Ratio Measurements of the SiO_2 or ZrO_2 Layers. The thickness of the SiO_2 or ZrO_2 layers formed either by the catalytic action of silicatein or silicatein/silintaphin around the nanowires was measured by analysis of TEM. A total of 10 nanowires were analyzed. For the ratios of Si/Ti and Zr/Ti in the nanowires, EDX (energy-dispersive X-ray spectroscopy) peak intensities for the elements Ti, Zr, and Si were evaluated for five nanowires in each sample (with one protein or with two proteins) and always in the middle of the nanowire in order for better comparison between samples. All measurements were made in triplicate, and the average of the measurements was taken. For statistical purposes, a paired Student's t test was applied.[43]

Atomic Force Miscropy (AFM) Analysis. Samples for AFM analysis were prepared by drop-casting: One drop from a 20 μL syringe of sample solution was deposited on a freshly cleaved mica surface. Subsequently, the mica sheet was transferred into a high-vacuum chamber and dried overnight. All SFM images were recorded at room temperature under ambient conditions using a commercial AFM (Multimode, Nanoscope IIIa controller, Veeco) in tapping mode. This instrument was equipped with a piezoelectric scanner allowing a maximum x,y-scan size of 17 μm and a maximum z-extension of 3.9 mm. Silicon cantilevers [OMCL AC240 and OMCL AC160 (Olympus), nominal spring constants of 2 and 42 N m^{-1}, and nominal resonance frequencies of 70 and 300 kHz, respectively] with an integrated tip and a tip radius <10 nm were plasma cleaned prior to use. Typically, the tip was scanned at velocities from 0.5 to 1 μm s^{-1}. For all samples, the topography and phase-contrast images were recorded. Raw data were modified by applying the first-order "flatten" filter in order to achieve scan lines at the same average height and average tilt.

RESULTS AND DISCUSSION

TiO_2 nanowires were used as backbone for the immobilization and subsequent coassembly of proteins and further to probe the influence of silintaphin-1 on the mineralization process. The TiO_2 nanowires were synthesized hydrothermally as described previously.[42] Further details on characterization of the nanowires can be found in the Supporting Information, Figure S2.

The functionalization of the TiO_2 nanowires was achieved by incubating the naked nanowires with the modified silicatein-α

dx.doi.org/10.1021/la200066q |*Langmuir* 2011, 27, 5464–5471

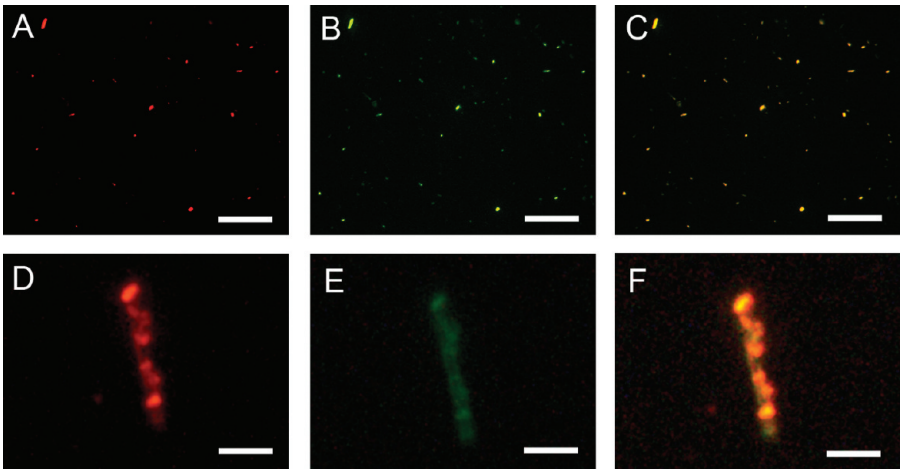

Figure 2. CLSM images of colocalization of silicatein-α and silintaphin-1. Immunocomplexes were visualized through treatment with secondary labeled antibodies with Cy3 (red) for silicatein-α or AlexaFluor 488 (green) for silintaphin-1. Overview and single nanowire functionalized with silicatein-α (A and D) and silintaphin-1 (B and E), respectively. Overlay image showing the colocalization of both proteins on the same nanowire (C and F). Scale bar in top row, 60 μm, and bottom row, 2 μm.

which possesses eight glutamate tags (Glu-tag, Figure 1A) in TBS buffer (Tris-buffered saline) at pH 7.4 for 2 h. Carboxylic groups have been shown previously to bind efficiently to metal oxides (particularly to titanium dioxide) surfaces, either by an ester-like linkage, bridging, or chelating with the metal centers on the surface, depending on the available surface coordination sites.[44,45] A scheme of the possible binding modes of Glu-tagged silicatein-α on TiO_2 surface is provided in Figure 1B.

The binding of Glu-tagged silicatein-α onto TiO_2 nanowires surface was monitored by confocal laser scanning microscopy (CLSM) using antisilicatein primary antibodies and fluorophore (Cy3) conjugated secondary antibodies. The CLSM image in Figure 2A shows that virtually every nanowire imaged emitted red fluorescence when excited using a 580 nm filter due to the presence of Cy3 fluorophore, and a higher magnification clearly reveals several protein−antibody coupled globular structures. As a control experiment, TiO_2 nanowires were incubated with normal recombinant histidine-tagged silicatein-α under a comparable set of conditions (TBS buffer, pH 7.4 for 2 h), where no fluorescence was observed (Supporting Information, Figure S3), thus proving that the binding of Glu-tagged silicatein-α to metal oxide surfaces is specific to the rich glutamate tag and not due to physical adsorption or nonspecific interactions with other protein domains.

In order to study the biospecific interaction of silintaphin-1 with silicatein in vitro, the TiO_2 nanowires functionalized with Glu-tagged silicatein-α were incubated with silintaphin-1 (in TBS buffer, pH 7.4, 50 μg/mL) for 1 h, accordingly with previous reported work.[18] Afterward, the presence of both silicatein-α and silintaphin-1 was monitored through immune-staining with specific primary antibodies for each protein and secondary antibodies labeled with different fluorophores (Cy3 for silicatein-α and AlexaFluor 488 for silintaphin-1). The Glu-tagged silicatein-α is present all over the nanowires (Figure 2A and D), as well as silintaphin-1 (Figure 2B,E), and an overlaid immunostained fluorescence image of the proteins on the TiO_2 nanowires shows a significant colocalization of both silicatein-α and silintaphin-1 on the surfaces, proving that the interaction has indeed occurred (Figure 2C,F).

In addition, to confirm the immobilization of silicatein and self-assembly of silintaphin-1 onto TiO_2 nanowires, atomic force microscopy (AFM) was performed on TiO_2 nanowires only with silicatein-α and with both silicatein-α and silintaphin-1. The AFM analysis of the as-synthesized TiO_2 nanowires (Figure 3A) showed a rather clean and smooth surface with an average roughness of 0.7 nm. The nanowires functionalized with Glu-tagged silicatein (Figure 3B) show a heterogeneous coating of protein with some possible protein aggregates, while the silicatein/silintaphin-1-functionalized nanowires show a more homogeneous distribution of protein on the surfaces due to the increase of organic matrix (Figure 3C).

To confirm that the immobilized Glu-tagged silicatein-α retains its catalytic activity toward the formation of silica and zirconia (as a proof of concept for the synthesis of a metal oxide layer), the TiO_2 nanowires functionalized with only Glu-tagged silicatein-α were incubated with a 5 mM solution of tetraethyl orthosilicate (TEOS) and potassium hexafluorozirconate (K_2ZrF_6) for 5 h at room temperature. As a control, bare nanowires were incubated with the above-mentioned precursor solutions under the otherwise identical conditions. In the latter case, no product was formed (data not shown). Subsequent TEM analysis revealed that the silicatein-α-functionalized nanowires are effectively decorated with silica and zirconia nanoaggregates, resulting in an inhomogeneous coverage of the material (Figure 4A,D). Images at higher resolution show the amorphous character of the silica domains. It is apparent that the thickness of deposited material is nonuniform over the length of the nanowires (Figure 4B,E). Higher-resolution micrographs show that the deposited zirconium dioxide is composed of nanoagglomerates over the complete sample. In addition, the presence of silica and zirconia was confirmed by EDX profiling of a single nanowire, where the elemental composition of the material shows the presence of Si or Zr, O, and Ti. Additional Cu peaks were detected due to the copper grids employed for sample analysis (Figure 4C,F).

Varying the concentration of precursors, either for silica or zirconia formation, or time of incubation did not vary considerably the aspect or thickness of the silica or metal oxide layer deposited over the length of the nanowires.

Hence, in order to achieve nanocomposites with characteristics closer to those found in nature, it is important to take into account the organic matrix present in vivo. The effect of interactors of silicatein-α on silica or metal oxides mineralization was studied using silintaphin-1, which was shown to bind to silicatein-α, even when

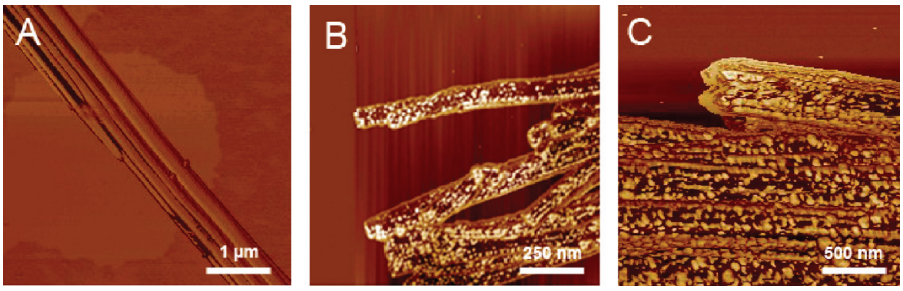

Figure 3. AFM phase-contrast images of TiO_2 nanowires: (A) as-synthesized, (B) with immobilized silicatein-α, and (C) with immobilized silicatein-α and silintaphin-1.

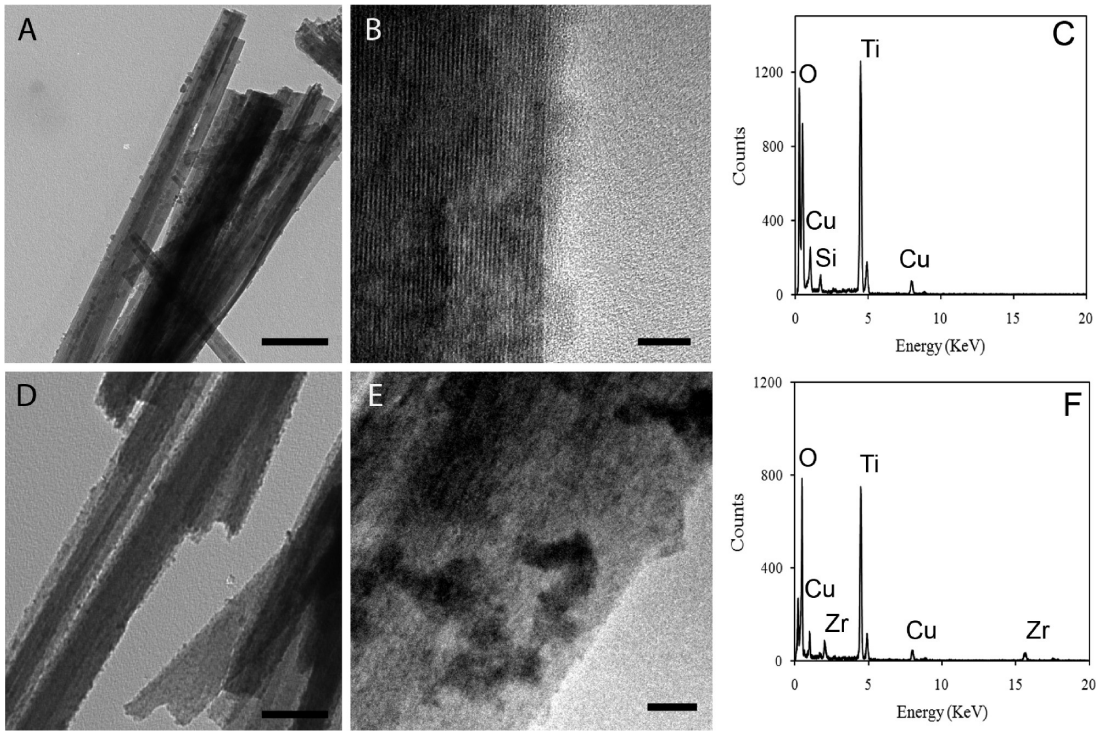

Figure 4. Formation of silica (A−C) or zirconia (D−F) by immobilized Glu-tagged silicatein-α on TiO_2 nanowires. (A) TEM overview image of TiO_2 nanowires covered with SiO_2 catalyzed by silicatein. (B) Higher magnification of the surface of TiO_2 nanowires covered with SiO_2. (C) EDX spectra of TiO_2 nanowires covered with SiO_2, thus indicating the presence of Ti, Si, and O. (D) TEM overview image of TiO_2 nanowires covered with ZrO_2 catalyzed by silicatein. (E) Higher magnification of TiO_2 nanowires covered with ZrO_2. (D) EDX spectra of TiO_2 nanowires covered with ZrO_2, thus indicating the presence of Ti, Zr, and O. Scale bars: (A) 100 nm, (B) 10 nm, (D) 50 nm, (E) 10 nm.

the later is immobilized on surfaces.[34] The binding mode of silicatein-α and silintaphin-1 is still under study. It is believed not to involve the active site of silicatein; i.e., usually one silicatein protein seems to interact with more than one silintaphin molecule.

As the interaction between silicatein-α and silintaphin-1 is not expected to be related with the active site of silicatein-α, the catalyzing effect toward the formation of silica and zirconia was tested as performed previously with Glu-tagged silicatein-α. Incubation of the functionalized TiO_2 nanowires with 5 mM solution (in TBS, pH 7.4) of either TEOS or potassium hexafluorozirconate was performed for 5 h at room temperature. As a control experiment, and to exclude a catalytic effect of silintaphin-1, TiO_2 nanowires were funtionalized only with silintaphin-1 (Supporting Information, Figure S4), with a polymeric ligand that binds histidine-tagged proteins to the surface of metal oxides, as described before (see Supporting Information for polymer synthesis and functionalization, Figure S1).[36] The silintaphin-1-functionalized nanowires were incubated under similar conditions with TEOS and potassium hexafluorozirconate.

The resulting composites were analyzed by transmission electron microscopy, as shown in Figure 5A,D. The silica-coated nanowires in the presence of both proteins show a layer with an uniform average thickness of 14.6 ± 3.9 nm, when compared with the coating obtain in the presence of silicatein only (Figure 4A), which only showed domains with an average thickness of about 6.4 ± 1.6 nm. High-resolution images of the silica−titania interface show the amorphous aspect as well as the uniform coverage over the complete surface (Figure 5B). Further EDX analysis confirms the presence of only Si, Ti, and O, as expected (Figure 5C).

For the ZrO_2-coated TiO_2 nanowires in the presence of both proteins, a thicker surface coverage was achieved (Figure 5D) in comparison with the coating using only silicatein (Figure 4D). The

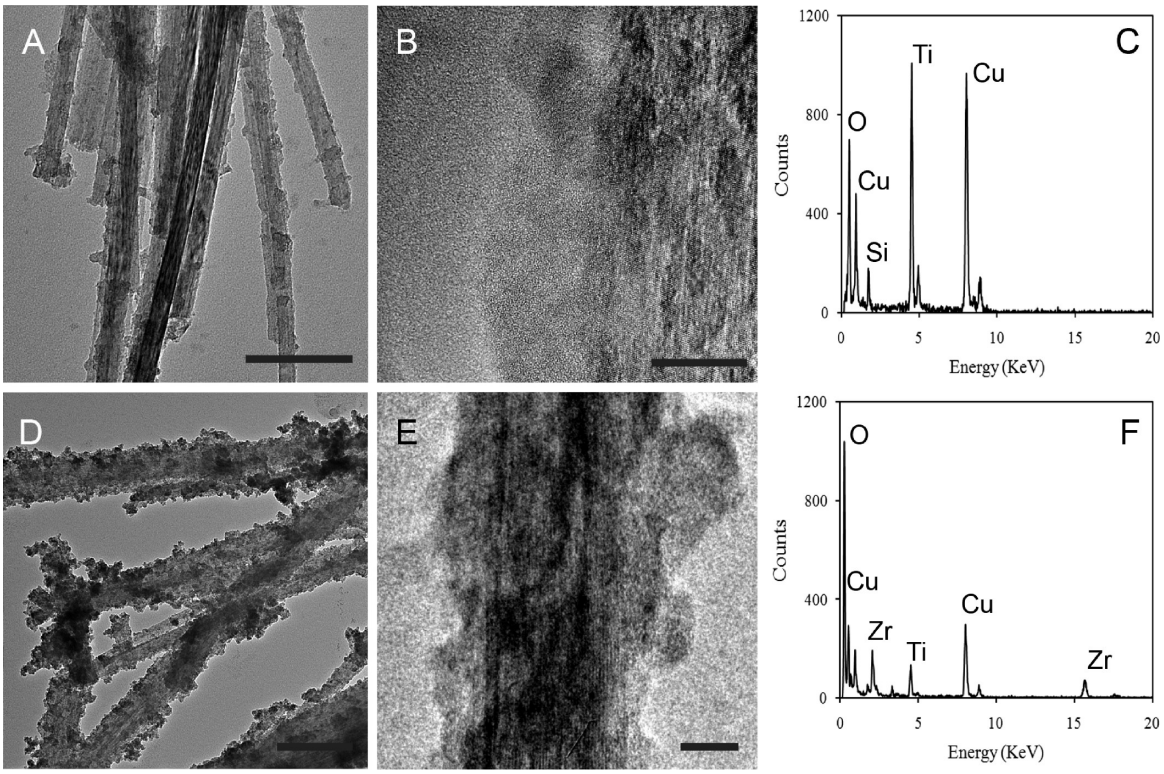

Figure 5. Formation of silica (A−C) or zirconia (D−F) by immobilized Glu-tagged silicatein-α and silintaphin-1 on TiO_2 nanowires. (A) TEM overview image of TiO_2 nanowires covered with SiO_2 catalyzed by silicatein/silintaphin. (B) Higher magnification of the surface of TiO_2 nanowires covered with SiO_2. (C) EDX spectra of TiO_2 nanowires covered with SiO_2, thus indicating the presence of Ti, Si, and O. (D) TEM overview image of TiO_2 nanowires covered with ZrO_2 catalyzed by silicatein/silintaphin. (E) Higher magnification of TiO_2 nanowires covered with ZrO_2. (D) EDX spectra of TiO_2 nanowires covered with ZrO_2, thus indicating the presence of Ti, Zr, and O. Scale bars: (A) 100 nm, (B) 10 nm, (D) 100 nm, (E) 10 nm.

average thickness of the ZrO_2 coating (in the presence of both proteins) was estimated to be around 22.2 ± 3.2 nm. In contrast, in the presence of only silicatein-α the average thickness was of 10.3 ± 2.1 nm. At higher resolution the increased thickness of the zirconia layer (Figure 5E) is clearly visible, as are crystalline domains with a fringe spacing of 2.96 Å [the (111) lattice spacing of cubic zirconia] were observed.[46] (Supporting Information, Figure S6B). These domains appear sparsely over the whole sample, but this is particularly interesting, as the high-temperature polymorph of zirconia can be synthesized under a physiological set of conditions (Supporting Information, Figure S6C).[47] EDX analysis shows the presence of Zr, Ti, and O, pointing to the presence of a zirconium dioxide layer on top of the titania nanowires (Cu peaks are due to the grid used for sample analysis) (Figure 5F).

Further quantification of the deposited layers of oxides using the different protein combinations was done through the analysis of EDX data by comparing the intensity for the Ti, Zr, and Si peaks in the EDX profiles. Values for comparison were made along several nanowires and averaged out. All measures were taken from the centers of the nanowires, in order to have comparable values, since the nanowires vary in diameter and length. Otherwise, as noted before, the mineralized coatings, especially for the silicatein/silintaphin samples, are homogenously deposited along the different nanowires (meaning no difference was observed, for example, between the middle and the tips of the nanowires).

The ratios of Si/Ti or Zr/Ti for the different samples are summarized in Table 1, where it is possible to confirm that higher amounts of either silica or zirconia are achieved, when both proteins where immobilized onto TiO_2 nanowires.

Table 1. Ratios of Si/Ti and Zr/Ti for the Samples Where either One Protein Was Used (silicatein) or Two Proteins Were Used (Silicatein/Silintaphin)[a]

sample	Si/Ti	Zr/Ti
silicatein	0.24 ± 0.10	0.31 ± 0.11
silicatein/silintaphin	0.74 ± 0.06	0.76 ± 0.10

[a] The values were obtained by evaluating the ration of the peak intensity detected by EDX in the different samples.

Thus it is shown that even though silintaphin-1 was added "on top" of silicatein-α, the active sites of silicatein-α are still available for catalyzing the formation of the oxides. The control experiment using TiO_2 nanowires functionalized with silintaphin-1 only showed no significant formation of either silica or zirconia (Supporting Information, Figure S5), which indicates that silintaphin-1 by itself has no catalytic effect on the formation of either silica or other metal oxides.

We can assume that when only one protein is present, a more heterogeneous organic layer is present, as seen in Figure 3B, and consequently, during mineralization also a heterogeneous coating is formed. On the other side, when both proteins are present a more homogeneous organic layer is present, resulting thus in a more homogeneous coating after mineralization.

The addition of silintaphin-1 led to the formation of a more uniform organic layer, which gives rise to a more homogeneous distribution of the oxide layer. Furthermore, silintaphin-1 is expected to have a synergistic effect toward silicatein-α, though not being active itself (as shown here; Supporting Information,

dx.doi.org/10.1021/la200066q |*Langmuir* 2011, 27, 5464–5471

Figure S5), by creating protein−protein aggregates, an interconnected network of proteins that is formed, allowing a more homogeneous mineralization.[18]

SUMMARY AND OUTLOOK

In summary, we have used the principles of surface functionalization, self-assembly, and enzyme catalysis to achieve a dense coating of TiO_2 nanowires with the metal oxides SiO_2 and ZrO_2. For this purpose we have used glutamate-tagged silicatein-α to functionalize the surface of TiO_2 nanowires. Silicatein-α retains its catalytic activity when immobilized on the surface of the nanowires. The surface-immobilized protein was shown to remain active by catalyzing the formation of silica and zirconia (as model metal oxides). Hence, it was shown that the direct immobilization of silicatein-α using incorporated surface specific tags is a simple and efficient method for one-step functionalization under mild physiological conditions (buffer solution, neutral pH, and at room temperature).

The tuning of the silica or metal oxide layer was further improved by the use of silintaphin-1, a silicatein-α interactor. It was shown that silintaphin-1 binds specifically to silicatein-α, even when the later is immobilized on a surface, and that silicatein-α still remains active toward the formation of metal oxides or silica. Silintaphin-1 by itself showed no noticeable catalytic effect toward the formation of these oxides.

The formation of silica or zirconia in the presence of both proteins produced a thick uniform surface coverage. Average coatings of 6.4 nm for silica and 14.6 nm for zirconia were obtained, over the whole sample when using both proteins. In contrast, attempts to fabricate homogeneous films with silicatein-α only produced a surface coverage with an average thickness of 10 nm for silica and 12 nm for zirconium dioxide under otherwise identical reaction conditions.

Hence, a fine-tuning of the formation of silica or zirconia by silicatein-α was achieved, which is of special interest in materials where surface properties at the nanoscale are of vital importance for the overall properties of the composites. Also, the synergistic effect of the several spicule protein matrix constituents was demonstrated, which may shed light into future work in the topic of artificial mineral formation.

ASSOCIATED CONTENT

Supporting Information. Polymer synthesis, synthesis and functionalization of the TiO_2 nanowires, TEM micrograph of as synthesized TiO_2 nanowires, optical and fluorescence microscopy images of the control experiments, CLSM images of Alexa488 fluorophore labeled silintaphin-1 immobilized on TiO_2, TEM images from control experiments with TiO_2 nanowires functionalized with silintaphin only, and high-resolution TEM images of zirconia-covered TiO_2 nanowires in the presence of silicatein-α and silintaphin-1. This material is available free of charge via the Internet at http://pubs.acs.org.

AUTHOR INFORMATION

Corresponding Author

*Phone: +49 6131 392-5135. Fax: +49 6131 392-5605. E-mail: tremel@uni-mainz.de.

ACKNOWLEDGMENT

This work was supported by the Deutsche Forschungsgemeinschaft (DFG) within the priority program 1420 "Biomimetic Materials Research" and the BMBF Center of Excellence BIOTEC Marin. The authors acknowledge support for the Electron Microscopy Center in Mainz (EZMZ) from the Center for Complex Matter (COMATT).

REFERENCES

(1) Daniel, M.-C.; Astruc, D. *Chem. Rev.* **2004**, *104*, 293–346.
(2) Talapin, D. V.; Lee, J.-S.; Kovalenko, M. V.; Shevchenko, E. V. *Chem. Rev.* **2010**, *110*, 389–458.
(3) Zhang, S. *Nat. Biotechnol.* **2003**, *21*, 1171–1178.
(4) Palmer, L. C.; Velichko, Y. S.; Olvera de la Cruz, M.; Stupp, S. I. *Philos. Trans. R. Soc. A* **2007**, *365*, 1417–1433.
(5) Lehn, J. M.; Ball, P. In *The New Chemistry*; Hall, N., Ed.; Cambridge Univ. Press: Cambridge, UK, 2000; pp 300−351.
(6) Desiraju, G. R. *Crystal Engineering: The Design of Organic Solids*; Elsevier: New York, 1989.
(7) Alberts, B.; Bray, D. ; Lewis, J.; Raff, M.; Roberts, K.; Watson, J. D. *Molecular Biology of the Cell*; Garland: New York, 1994.
(8) Sahoo, J. K.; Tahir, M. N.; Yella, A.; Schladt, T. D.; Mugnaioli, E.; Kolb, U.; Tremel, W. *Angew. Chem.* **2010**, *120*, 7741–7745; *Angew. Chem., Int. Ed.* **2010**, *49*, 7578–7582.
(9) Hall, S. R. *Proc. R. Soc. A* **2009**, *465*, 335–366.
(10) Bushan, B. *Philos. Trans. R. Soc. A* **2009**, *367*, 1445–1486.
(11) Lakes, R. *Nature* **1993**, *361*, 511–515.
(12) Zhang, S.; Marini, D. M.; Hwang, W.; Santoso, S. *Curr. Opin. Chem. Biol.* **2002**, *6*, 865–871.
(13) Cattaneo-Vietti, R.; Bavstrello, G.; Cerrano, C.; Sara, M.; Benatti, U.; Giovine, M.; Gaino, E. *Nature* **1996**, *383*, 397–398.
(14) Weiner, S.; Wagner, H. D. *Annu. Rev. Mater. Sci.* **1998**, *28*, 271–298.
(15) Aizenberg, J.; Weaver, J. C.; Thanawala, M. S.; Sundar, V. C.; Morse, D. E.; Fratzl, P. *Science* **2005**, *309*, 275–278.
(16) (a) Cha, J. N.; Shimizu, K.; Zhou, Y.; Christiansen, S. C.; Chmelka, B. F.; Stucky, G. D.; Morse, D. E. *Proc. Natl. Acad. Sci. U. S. A.* **1999**, *96*, 361–365. (b) Schröder, H. C.; Boreiko, A.; Korzhev, M.; Krasko, A.; Tahir, M. N.; Tremel, W.; Eckert, C.; Müller, I. M.; Müller., W. E. G. *J. Biol. Chem.* **2006**, *281*, 12001–12009.
(17) Imhoff, J. M.; Garrone, R. *Connect. Tissue Res.* **1983**, *11*, 193–197.
(18) Wiens, M.; Bausen, M.; Natalio, F.; Link, T.; Schlossmacher, U.; Müller, W. E. G. *Biomaterials* **2009**, *30*, 1648–1656.
(19) Müller, W. E. G.; Belikov, S. I.; Tremel, W.; Gamulin, V.; Perry, C. C.; Boreiko, A.; Schröder, H. C. *Micron* **2006**, *37*, 107–120.
(20) Müller, W. E. G.; Rothenberger, M.; Boreiko, A.; Tremel, W.; Reiber, A.; Schröder, H. C. *Cell Tissue Res.* **2005**, *321*, 285–297.
(21) Uriz, M. J.; Turon, X.; Becerro, M. A. *Cell Tissue Res.* **2000**, *301*, 299–309.
(22) Sumerel, J. L.; Yang, W.; Kisailus, D.; Weaver, J.; Choi, J. H.; Morse, D. E. *Chem. Mater.* **2003**, *15*, 4804–4809.
(23) Mueller, W. E. G.; Wang, X. H.; Kropf, K.; Ushijima, H.; Geurtsen, W.; Eckert, C.; Tahir, M. N.; Tremel, W; Boreiko, A.; Schlossmacher, U.; Li, J.; Schroeder, H. C. *J. Struct. Biol.* **2008**, *161*, 188–203.
(24) Tahir, M. N.; Théato, P.; Müller, W. E. G.; Schröder, H. C.; Boreijko, A.; Faiss, S.; Janshoff, A.; Huth, J.; Tremel, W. *Chem. Commun.* **2005**, *28*, 5533–5535.
(25) Kisailus, D.; Choi, J. H.; Weaver, J. C.; Yang, W.; Morse, D. E. *Adv. Mater.* **2005**, *17*, 314–318.
(26) Brutchey, R. L.; Morse, D. E. *Chem. Rev.* **2008**, *108*, 4915–4934.
(27) Aizenberg, J.; Sundar, V. C.; Yablon, A. D.; Weaver, J. C.; Chen, G. *Proc. Natl. Acad. Sci. U. S. A.* **2004**, *101*, 3358–3363.
(28) Müller, W. E. G.; Wendt, K.; Geppert, C.; Wiens, M.; Reiber, A.; Schröder, H. C. *Biosens. Bioelectron.* **2006**, *21*, 1149–1155.
(29) Cha, J. N.; Shimizu, K.; Zhou, Y.; Christiansen, S. C.; Chmelka, B. F.; Stucky, G. D.; Morse, D. E. *Proc. Natl. Acad. Sci. U. S. A.* **1999**, *96*, 361–365.

(30) Shimizu, K.; Cha, J.; Stucky, G. D.; Morse, D. E. *Proc. Natl. Acad. Sci. U. S. A.* **1998**, *95*, 6234–6238.
(31) Bartlett, J. D.; Ganss, B.; Goldberg, M.; Moradian-Oldak, J.; Paine, M. L.; Snead, M. L.; Wen, X.; White, S. N.; Zhou, Y. L. *Curr. Top. Dev. Biol.* **2006**, *74*, 57–115.
(32) Dominguez, R.; Holmes, K. C. *Annu. Rev. Biophys.* **2011**in press.
(33) Rivas, J. De Las; Fonatanillo, C. *PLoS Comput. Biol.* **2010**, *6*, e1000807.
(34) Krasko, A.; Batel, R.; Schröder, H. C.; Müller, I. M.; Müller, W. E. G. *Eur. J. Biochem.* **2000**, *267*, 4878–4887.
(35) Tahir, M. N.; Théato, P.; Müller, W. E.G.; Schröder, H. C.; Janshoff, A.; Zhang, J.; Huth, J.; Tremel, W. *Chem. Commun.* **2004**, 2848–2849.
(36) Tahir, M. N.; Eberhardt, M.; Therese, H. A.; Kolb, U.; Theato, P.; Müller, W. E. G.; Schröder, H. C.; Tremel, W. *Angew. Chem.* **2006**, *118*, 4921–4927; *Angew. Chem., Int. Ed.* **2006**, *45*, 4803–4809.
(37) Schröder, H. C.; Natalio, F.; Shukoor, I.; Tremel, W.; Schlossmacher, U.; Wang, X.; Müller, W. E. G. *J. Struct. Biol.* **2007**, *159*, 325–334.
(38) Shukoor, M. I.; Natalio, F.; Tahir, M. N.; Metz, N.; Ksenofontov, V.; Theato, P.; Schröder, H. C.; Müller, W. E. G.; Tremel, W. *Chem. Mater.* **2008**, *20*, 3567–3573.
(39) Shukoor, M. I.; Natalio, F.; Krasko, A.; Schröder, H. C.; Müller, W. E. G.; Tremel, W. *Chem. Commun.* **2007**, 4677–4679.
(40) Shukoor, M. I.; Natalio, F.; Glube, N.; Tahir, M. N.; Therese, H. A.; Ksenofontov, V.; Metz, N.; Theato, P.; Langguth, P.; Boissel, J.-P.; Schröder, H. C.; Müller, W. E. G.; Tremel, W. *Angew. Chem.* **2008**, *120*, 4826–4830; *Angew. Chem., Int. Ed.* **2008**, *47*, 4748–4752.
(41) Natalio, F.; Link, T.; Müller, W. E. G.; Schröder, H. C.; Cui, F.; Wang, X.; Wiens, M. *Acta Biomater.* **2010**, *6*, 3720–3728.
(42) Armstrong, A. R.; Armstrong, G.; Canales, J.; Bruce, P. G. *Angew. Chem.* **2004**, *116*, 2336–2338; *Angew. Chem., Int. Ed.* **2004**, *43*, 2286–2288.
(43) Sachs, L. *Angewandte Statistik*; Springer: Berlin, 1984, 242−243.
(44) Umland, F.; Wünsch, G. *Charakteristische Reaktionen Anorganischer Stoffe*, 2nd ed.; Aula Verlag: Wiesbaden, 1991.
(45) Kaim, W.; Schwederski, B. *Bioanorganische Chemie: Zur Funktion Chemischer Elemente in Lebensprozessen*, 4th ed.; Teubner: Stuttgart, 2005.
(46) Tahir, M. N.; Gorgishvili, L.; Li, J.; Gorelik, T.; Kolb, U.; Nasdala, L.; Tremel, W. *Solid State Sci.* **2007**, *9*, 1105–1109.
(47) Navrotsky, A. *Geochem. Trans.* **2003**, *4*, 34–37.